NANO LETTERS

Letter

pubs.acs.org/NanoLett

A Close Look at Proteins: Submolecular Resolution of Two- and Three-Dimensionally Folded Cytochrome c at Surfaces

Zhitao Deng,[†] Nicha Thontasen,[†] Nikola Malinowski,[†] Gordon Rinke,[†] Ludger Harnau,[‡,¶] Stephan Rauschenbach,*[,†] and Klaus Kern[†,§]

[†]Max-Planck-Institute for Solid State Research, Heisenbergstrasse 1, D-70569 Stuttgart, Germany

[‡]Max-Planck-Institute for Intelligent Systems, Heisenbergstrasse 3, D-70569 Stuttgart, Germany

[¶]Institut für Theoretische und Angewandte Physik, Universität Stuttgart, Pfaffenwaldring 57, 70569 Stuttgart, Germany

[§]Institut de Physique de la Matière Condensée, Ecole Polytechnique Fédérale de Lausanne, CH-1015 Lausanne, Switzerland

S *Supporting Information*

ABSTRACT: Imaging of individual protein molecules at the single amino acid level has so far not been possible due to the incompatibility of proteins with the vacuum environment necessary for high-resolution scanning probe microscopy. Here we demonstrate electrospray ion beam deposition of selectively folded and unfolded cytochrome c protein ions on atomically defined solid surfaces in ultrahigh vacuum (10^{-10} mbar) and achieve unprecedented resolution with scanning tunneling microscopy. On the surface folded proteins are found to retain their three-dimensional structure. Unfolded proteins are observed as extended polymer strands displaying submolecular features with resolution at the amino acid level. On weakly interacting surfaces, unfolded proteins refold into flat, irregular patches composed of individual molecules. This suggests the possibility of two-dimensionally confined folding of peptides of an appropriate sequence into regular two-dimensional structures as a new approach toward functional molecular surface coatings.

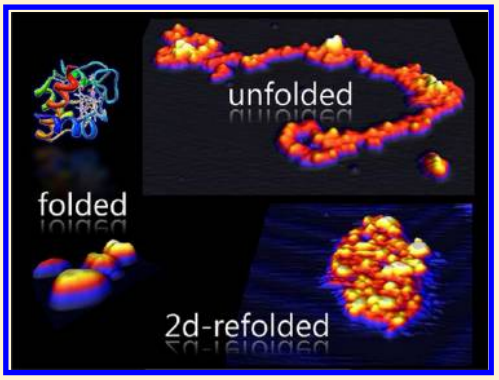

KEYWORDS: *Ion beam deposition, proteins, scanning tunneling microscopy, amino acid, folding, soft landing*

Proteins, macromolecules of almost unmatched complexity, display highly specific functionalities only when folded into a distinct three-dimensional (3D) configuration. Protein folding, a complex self-assembly process, thus links the protein's functionality to the atomic arrangement of the peptide chain.[1,2] Consequently the protein's 3D shape as well as its peptide sequence are of pivotal importance for the understanding of the processes in the living cell. Moreover, due to their exquisite functionalities, proteins are very interesting for the applications in biotechnology. Especially the immobilization of proteins at surfaces, controlled with respect to structure and ordering, is of great importance.[3]

Electrospray ionization (ESI) produces intact protein gas-phase ions, which allows to employ mass spectrometry for the identification and sequencing of biological molecules like proteins with great precision.[4] However, from gas-phase protein ions, only limited information about the complex 3D structure can be extracted by ion mobility spectrometry (IMS), which condenses the complexity of the protein's shape to just one number, the collision cross section.[5,6]

While the identification and sequencing of proteins is very efficiently done using modern mass spectrometry techniques,[7] the imaging of the 3D shape of a protein is a highly complex task, which remains a challenge on the individual particle scale. Averaging over many molecules of a protein crystal, X-ray crystallography is the conventional method, allowing for a high-resolution determination of the atomic positions.[8] The preparation of protein crystals however, is often tedious—sometimes impossible. Alternatively, the computational alignment and averaging of many transmission electron micrographs of the same protein for tomographic reconstruction yield submolecular resolution of its 3D shape, yet requires similarly large efforts.[9,10]

Scanning probe microscopy (SPM) is capable of achieving atomic resolution and should in principle be capable of imaging individual proteins at this resolution.[11,12] However, only on atomically clean samples, preferably in an ultrahigh vacuum (UHV) environment to avoid any contamination, molecular orbital or even atomic resolution of an adsorbate molecule can be achieved.[13] Since proteins, in particular in the folded state, are delicate with respect to environmental influences like heat, lack of water, or ill solvent conditions, their processing is limited to solutions or ambient conditions. Thus vacuum processing by thermal evaporation that could produce well-defined samples for high-resolution SPM imaging is hindered by the nonvolatile nature of proteins.

Received: February 8, 2012
Revised: April 10, 2012

   dx.doi.org/10.1021/nl3005385 | *Nano Lett.* XXXX, XXX, XXX−XXX

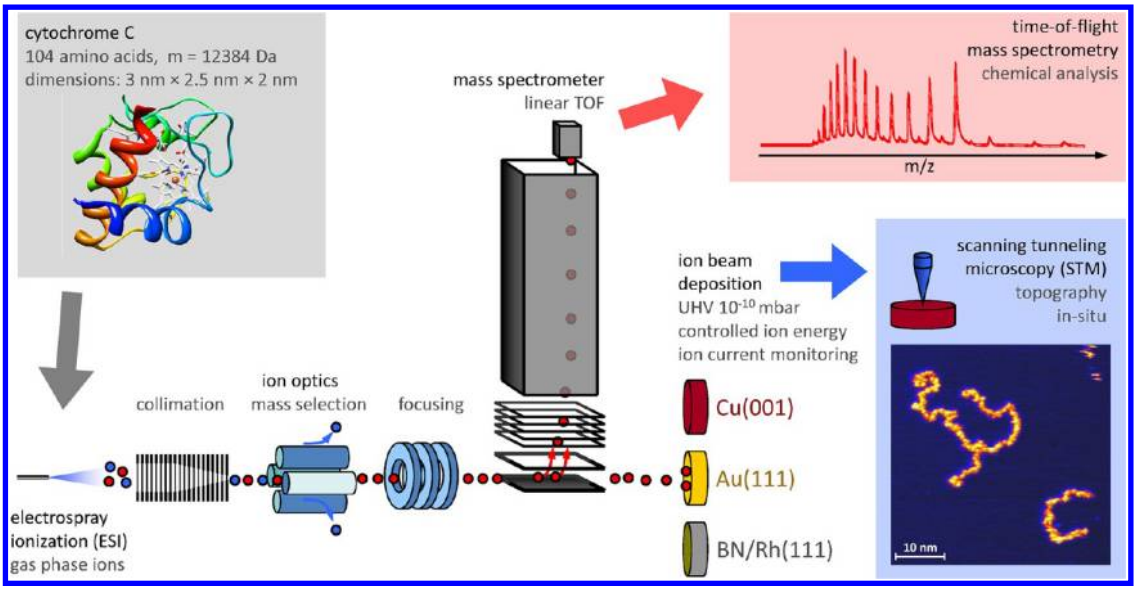

Figure 1. Scheme of the ES-IBD experiment. The protein CytC, displayed in ribbon representation, is ionized by ESI. Ion optics, such as an ion funnel, quadrupoles, and lenses are used to collimate, mass select, and focus the beam. TOF-MS allows access to the chemical composition. Ion beam deposition takes place in ultrahigh vacuum (10^{-10} mbar). The deposition energy can be adjusted, and the ion current is monitored. Samples are investigated in situ by STM (see Supporting Information A for details).

In this study we are aiming at the characterization of individual proteins on surfaces by STM at the amino acid resolution level. To place the molecules on atomically defined crystalline surfaces in UHV, we use electrospray ion beam deposition (ES-IBD), a technique also known as ion soft landing.[14−19] Similar to atoms or small molecules from an evaporator source used in conventional molecular beam epitaxy, our advanced ES-IBD setup generates intact molecular gas-phase ions through ESI and conveys them as fully controlled, highly pure ion beams to surfaces in UHV.[20−22] With this approach, folded or unfolded proteins can be deposited selectively by specifically acidifying the electrospray solution and filtering appropriate low- or high-charge states, respectively.

Soft landing of proteins has been demonstrated in high vacuum.[23] It was demonstrated that the protein functionality can be retained[16,24] and that even complex entities like whole viruses can be deposited intactly.[25] Since the deposition process itself is highly complex, the detailed picture of surfaces coated with proteins by ES-IBD/soft landing will allow to optimize that process toward applications of selectively coated functional protein surfaces.

In the following we show that folded proteins were deposited intact on metal surfaces in vacuum and, despite their large size and insulating nature, can be imaged by STM as globular structures. For unfolded proteins, we achieved the mapping of the electronic density of states with submolecular resolution at the amino acid level. This enables us to study the complex interaction of the peptide strands with the surface and probe their microscopic properties and self-assembly behavior. Steered by the interaction with the surface, we obtain different structures that could be useful for approaching various questions: We will show that protein ions, fully immobilized upon deposition, yield information about the gas-phase ion's conformation with unprecedented resolution. Submolecular features related to single or few amino acids (AA) observed along extended unfolded protein strands suggest to probe the AA sequence by scanning probe spectroscopy. Two-dimensional (2D) folding into disordered compact patches was found, which suggests a surface confined, 2D equivalent to protein folding as a new approach toward complex, functional surface coatings.

Like in mass spectrometry, in ES-IBD molecular ions created by ESI are transferred into vacuum and proceed through several ion optics for collimation, mass selection, and focusing before they can be detected with the mass spectrometer or used for deposition onto a surface (Figure 1).[20,23] The feasibility of ES-IBD for intact deposition has been demonstrated in several cases including peptides,[26,27] dye molecules,[20,28] coordination compounds,[21,29] fragile molecular magnets,[22,30] and even whole viruses.[25] The gentle deposition of protein ions on liquid and solid surfaces in vacuum has been reported to be capable of retaining the functionality of the molecule.[16,24] With the prototype of our ES-IBD setup, nanostructures of bovine serum albumine (BSA), a large protein, were formed on a graphite surface in high vacuum (10^{-6} mbar).[23] The ambient condition characterization with atomic force microscopy (AFM), however, was limited in resolution to the level of the single globule, of 1−5 nm in diameter.

In the present study, we investigate cytochrome c (CytC), a protein central in electron-transfer processes in mitochondria and in apoptosis.[31] It consists of 104 AA adding up to a molecular weight of 12 384 Da.[32] For comparison, BSA, a protein of more then 66 kDa mass, is studied.[23] ESI charges proteins by the addition of multiple protons, a process which can be enhanced by acidifying the solution, e.g., with formic acid (FA).[33] Figure 2a shows mass spectra of CytC from aqueous solutions that contain 0.1% and from H_2O/MeOH solutions containing 5% FA. The characteristic peak pattern corresponds to several charge states of CytC: +5 to +12 are detected at low FA concentration (blue curve). Upon increasing the FA concentration to 5% and adding the organic solvent, the characteristic red color of the solution vanishes, indicative of protein denaturation. TOF-MS yields higher charge states of up to +20 (Figure 2a, red curve). Still, the mass

dx.doi.org/10.1021/nl3005385 | Nano Lett. XXXX, XXX, XXX−XXX

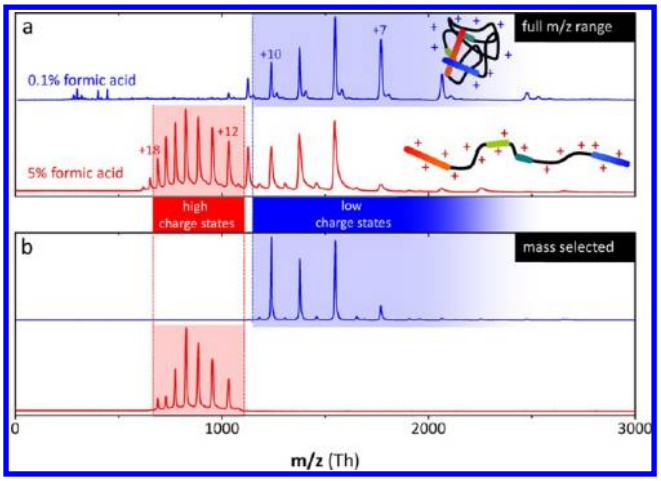

Figure 2. Electrospray TOF-MS of equine CytC from an aqueous solution containing 0.1% FA (blue) and from a H_2O/MeOH solution with 5% FA added (red): (a) without mass selection low-charge states from +5 to +12 are found for low FA concentration. High-charge states up to +20 are observed for high FA concentration. (b) Mass selection of high- (z = +12 to +18) and low- (z < +10) charge states yields beams that contain preferably unfolded or folded protein ions, respectively.

of (12 385 ± 6) Da measured confirms that the CytC molecules are intact.

The relation between the charge state of the gas-phase ion and the conformation of the protein has been intensively studied for CytC by measuring ion-neutral collision cross sections and examining H/D exchange studies.[34−36] The results suggest two main conformational states: unfolded proteins preferably form high-charge state ions (z > +10), while folded and partially unfolded proteins are found in low-charge states (z < +8). ES-IBD thus offers to choose the type of protein conformer to deposit by adjusting the solution conditions to promote folded or unfolded proteins, and select the m/z range of the desired charge states.

To explore the molecular structure of individual folded and unfolded proteins at surfaces, beams of high- and low-charge state were prepared for deposition. This was achieved by mass selecting the ranges of 600−1200 Th (z = +12 to +18) and m/z > 1250 Th ($z \leq$ +10) with a quadrupole ion guide in addition to the adjustment of the pH value (see Figure 2b). For the UHV deposition, currents of 15−60 pA can be achieved at the target, which relate to a deposition time of 0.5−3 h for a submonolayer coverage of 5−20% of the total surface area, which is ideal for the investigation of the individual molecules by STM. Higher coverage can be achieved by collecting more charge, with results equivalent to low coverage imaging. However, the imaging quality is reduced as the films become more and more insulating.

Low-charge state, folded CytC beams were deposited on three surfaces (for details see Supporting Information A). Cu(001) is a strongly interacting surface, on which the molecules are expected to be fully immobilized already at room temperature. Au(111) is less interactive, except at the elbow sites of the reconstruction, which act as pinning centers.[37] Finally an insulating, monatomic boron-nitride nanomesh (BN) layer on Rh(111) interacts weakly, yet offers a regularly modulated surface of approximately 3.2 nm pitch, which can serve as a template for ordered organization.[38]

Figure 3 shows the three surfaces after the deposition of a submonolayer coverage of low-charge state, folded CytC ions.

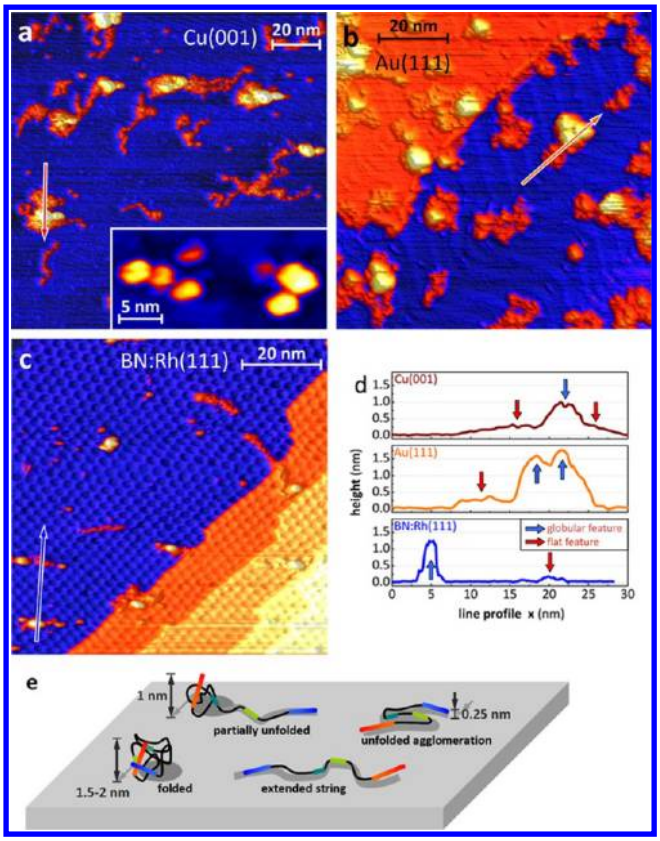

Figure 3. STM topography of folded proteins after the deposition of low-charge state CytC ion beams: (a) on Cu(001); inset: individual globular features at improved resolution due to a modified tip; (b) on Au(111); and (c) on BN/Rh(111) boron nitride nanomesh. (d) Line profiles showing completely and partially folded proteins as high (1.0−1.8 nm), globular features, and unfolded proteins as features of low height (0.2−0.3 nm). (e) Sketch of possible protein configurations: several nanometer high features result from partially or completely folded proteins, flat laying strings, or patches correspond to unfolded protein strands.

On all surfaces two types of structural features can be distinguished: (i) high, globular structures of 1.0−1.8 nm apparent height, with lateral dimensions of 2−4 nm and (ii) low height, string-like features on Cu and BN or patches on Au with a height of 0.2−0.3 nm (see line profiles, Figure 3d). It is evident that the strings found on Cu(001) and BN correspond to unfolded protein strands, which on Au(111) agglomerated into compact patches.

To identify the nature of the globular features, the entire deposition and imaging process has to be considered, as both random coils or folded proteins are possible explanations for the observed structures. In STM large organic structures appear less high due to a lower electronic density of states as compared to the metal, while the lateral dimensions of high aspect ratio structures are overestimated due to the convolution with the tip shape. Taking into account these limitations imposed by the STM imaging method, the structures resemble the shape and size of the three-dimensionally folded CytC[39] fairly well, while for random coils a larger variety of shapes could be expected. According to IMS studies, our ion beam of low-charge state CytC ions contains folded along with partially and completely

dx.doi.org/10.1021/nl3005385 | Nano Lett. XXXX, XXX, XXX−XXX

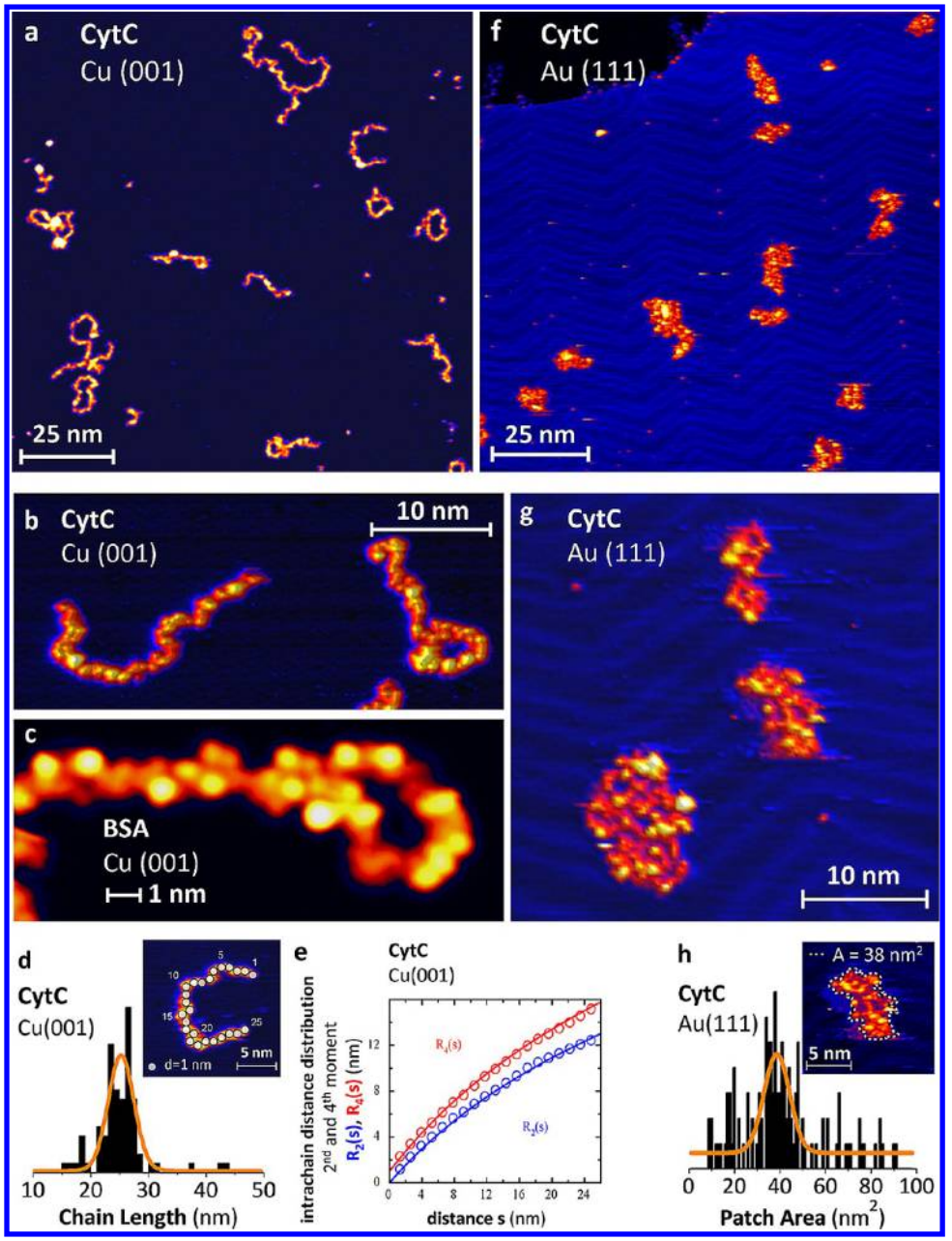

Figure 4. STM topographies of unfolded CytC deposited from ion beams of high-charge state: (a) CytC on Cu(001), large scale image and (b) magnified topograph showing two peptide stands on Cu(001) with molecular substructure. (c) Other proteins, here BSA, reproduce equivalent structural features on Cu(001). High-resolution topograph of a section of an unfolded BSA molecule showing lobes separated by 0.5−0.8 nm along the chain. (d) Histogram of the chain length on Cu(001) yielding an average of 25 ± 3 nm, which fits an unfolded protein with intact α-helices. (e) The second and fourth moment of the intrachain distance measured from STM images (hollow circles) fits the predictions of a worm-like chain model for a noninteracting polymer (straight lines). $R_4(s)$ data shifted by 1 for clarity. (f) Unfolded CytC on Au(111). (g) Magnification of compact patches of CytC. Two small patches of approximately 40 nm^2 represent one protein each, the large patch of 80 nm^2 comprises two strands. (h) The histogram of the patch area. Feature heights in panels a−c 0.15−0.25 nm and for panels f, g 0.15−0.35 nm.

unfolded proteins.[34,36] Refolding of unfolded protein strands in the gas phase is unlikely due to the short transfer time between ionization and deposition and was further avoided by choosing gentle conditions in the high-pressure part of the ion source where collisions with the background gas occur.[40,41] That this is successful, is evidenced by the absence of globular features in experiments with purely unfolded beams (see Figure 4) and it further shows that refolding into globular structures does not occur on the surface either.

Thus the different structures observed by STM after the deposition of low-charge state CytC ion beams can be rationalized by the configurations illustrated in Figure 3e: Globular features of heights above 1 nm are observed where a folded or partially folded protein is present, while the features of 0.15−0.35 nm height correspond to unfolded proteins appearing as isolated, strand- or patch-like agglomerations. Partially unfolded proteins are imaged as a mixture of flat and globular structures in the vicinity of each other. We note that, as a consequence of the transfer into vacuum, the intramolecular interactions in the protein are altered due to the removal of the solvent. The missing hydrophobic interaction stabilizes the protein's secondary structure through stronger

dx.doi.org/10.1021/nl3005385 | Nano Lett. XXXX, XXX, XXX−XXX

polar interactions and the electrostatic repulsion results in a set of folded conformers that is expected to be close yet not equal to the folded protein in solution.[36,42]

While we can exclude refolding of unfolded strands into globular structures mediated by the surface, an influence on the molecular ion's conformation on the distribution of the deposited material is obvious. Our low-charge state ion beam collides at an energy of 10−50 eV with the surface. For this energy range former protein soft-landing studies reported enzymatic activity after deposition, which suggests that a significant amount of folded proteins survives the impact.[16,24] Unfolding as a consequence of the contact to the metal or BN surface seems unlikely as well, since a similar ratio of folded and unfolded proteins is found either on the strongly interacting Cu(001) surface or on weakly interacting Au(111) and BN surfaces. However, since in the low-charge state ion beam folded and unfolded proteins are present, the unfolding due to the impact or due to the surface cannot be dismissed entirely.

On Cu(001) the CytC molecules are immobilized where they have landed. At room temperature, almost no step edge decoration is observed on Cu(001), indicative of inhibited diffusion. Few, small agglomerations of globular features suggest some surface mobility for folded as compared to unfolded proteins (see inset of Figure 3a and Figure 3b). Intuitively, the smaller contact area of the surface with a folded protein rationalizes this observation.

On the less interactive Au(111) and BN surfaces, STM measurements have to be performed at low temperature (40 K) to reduce the surface mobility enough to observe individual proteins. Step edges and the elbow sites of the Au(111) reconstruction act as pinning centers, where folded and unfolded molecules are found. The surface mobility also accounts for the observation of the compact patches that can be better observed when only unfolded proteins are deposited, which is discussed in detail later. In contrast to Au(111), the BN nanomesh reconstruction provides a template of much smaller length scale, trapping the molecules on the terraces and moreover limiting the free motion of the unfolded protein strands, which hinders the formation of compact patches.

The considerations above suggest that the folded proteins are not strongly perturbed by the adsorption at the surface. Unfortunately, the relatively large height of the globular structures combined with their insulating nature induces frequent contact with the STM tip, i.e., the tip crashes. As a consequence, the tunneling junction is not always well-defined, often reducing image resolution and quality. A newly prepared tip, for instance, would image the unfolded strands with good resolution and show fuzzy protrusions at the sites of the globules. A tip that sometimes gets modified by the attachment of a molecule may resolve the individual folded proteins, while the unfolded strands are imaged badly (see inset of Figure 3a).

In the absence of the folded proteins, much better tunneling conditions would allow for molecular orbital resolved imaging by STM. Since ES-IBD promotes isolating high-charge state ions by mass selection (see Figure 2b, red spectra), we deposited purely unfolded proteins to the surface, exposing the entire molecule to be imaged by the STM. Moreover, the self-assembly behavior of a peptide chain on the surface, governed by complex intermolecular, intramolecular and molecule-surface interactions, is fundamentally interesting and may serve as a new way to fabricate surface supported nanostructures. In principle, the manifold of interactions promotes self-assembly at a surface given sufficient mobility, whereas the folding into a 3D structure or even into the protein seems highly unlikely to occur due to the binding to the metal surface.

The results of the deposition of high-charge states resemble the observations after the deposition of low-charge state ions but with the globular structures entirely absent. String-shaped adsorbates are observed on the otherwise clean Cu(001) surface after the deposition of a 0.05 ML coverage of high-charge state CytC ($z \geq 12$) (Figure 4a,b). A statistical analysis yields a length of 25 ± 3 nm (Figure 4d), which is significantly shorter than the expected length of 35.5 nm of the entirely unfolded protein. Considering, however, that the high stability of the secondary structure in vacuum leads to intact α-helices,[43,44] the expected length is 27 nm, which agrees well with our observation. Moreover the narrow length distribution shows that unfolded highly charged proteins are soft landed at energies of up to 90 eV, which is in agreement with the literture on the topic.[16,19,24]

On Cu(001) at room temperature, no pair of CytC molecules with the exact same adsorption configuration can be found. The flexibility of the polymer chain allows for an enormous number of possible configurations in three dimensions. The same is true even when the confinement to a surface reduces the degrees of freedom. The formation of the observed random structures cannot be attributed to thermal diffusion or collision induced motion since no sign of surface mobility, such as step edge decoration, agglomeration, or molecular ordering, is found for purely unfolded CytC on Cu(001). We conclude that unfolded CytC protein ions are immobilized immediately upon contact with the strongly interacting Cu(001) surface. Due to it is softness, the gas-phase structure is only weakly perturbed by the strain induced by the collision with the surface. The observed geometry thus is a close approximation of the gas-phase ion's configuration projected to the surface.

Caused by Coulomb repulsion, highly charged protein ions, without disulfide bonds like CytC, have an extended chain conformation in the gas phase. To justify this argumentation, we have performed molecular dynamics simulations of CytC in vacuum. The calculated characteristic conformations of highly charged CytC are indeed similar to the ones shown in Figure 4a,b (Supporting Information E, Figure S4). Our data from the analysis of the distribution of intramolecular distances on the surface match the behavior of a 3D worm-like chain, with a persistence length of 6 nm, projected onto a surface (see Figure 4e and Supporting Information B).[45] Since this model does not take the AA sequence into account, it predicts the general behavior of unfolded proteins on the Cu(001) surface. And even though the full complexity of the protein deposition process, including hyperthermic energies and the mechanical properties of the peptide, is not reflected by our model, the structures observed for the much larger protein BSA resemble what we find for CytC and confirm the application of the wormlike chain model (Figure 4c and Supporting Information D).

In contrast to the extended chains observed on Cu(001), after the deposition of high-charge state CytC ion beams on Au(111), compact patches corresponding to individual molecules, covering an area of approximately 39 ± 4 nm^2, are observed (Figure 4f,g). They are found at the step edges and at the elbow sites of the reconstruction, indicating surface mobility of the unfolded protein stands on gold. These flat, compact structures are the result of attractive intramolecular interactions. In contrast to the gas phase, on a metal surface charged sites are

dx.doi.org/10.1021/nl3005385 | Nano Lett. XXXX, XXX, XXX−XXX

either neutralized or effectively screened. While initially the protein binds at one or only few points, for instance, via opened disulfide bonds or a carboxylic acid group binding strongly to the gold, the rest of the chain remains mobile. It will be fully immobilized at an energetically favorable position, which is most likely in the vicinity of another part of the same chain. The characteristic pseudodiameter of these patches in the plane of the Au(111) surface is determined by the aforementioned persistence length of the unfolded CytC proteins. This mechanism is sufficient to explain the occurrence of irregular patches and suggests that the intrachain interactions are nonspecific, since no identical patches are found.

Without disturbances imposed by the large insulating globules, a better resolution can be achieved compared to the STM measurements of folded proteins. The primary structure of CytC is imaged as a set of protrusions. The height of the patch structures on Au(111) of 0.15−0.35 nm is found to be higher than the height of the string-shaped adsorbates on Cu(100) of 0.15−0.25 nm. In the close-packed patches, not all side groups of the AAs are laying flat on surface. Protrusions above 0.3 nm height are thus attributed to the side groups of AAs pointing out of the surface plane. Individual peptide chains on Cu(001) are shown in Figure 4b,c, each composed of many protrusions of varying size (or pitch equivalently) of 0.5−0.8 nm. This length, measured for BSA as well as for CytC, corresponds to the size of one to three AAs. Accordingly, the number of 30−60 lobes is found to be a fraction of the number of 104 AAs for CytC. On Au(111) the distribution and size of submolecular protrusions are consistent with CytC on copper. However, since the CytC chain interacts with itself, the number of observed protrusions is reduced to 20−30 per patch. The variation of the intensity in the lobes is related to the local density of states, which depends on the AA sequence.

Our results show that ES-IBD is a method to efficiently prepare high-quality surfaces selectively coated with unfolded as well as folded proteins. Such samples can be useful for many high-performance measurement methods targeting fragile, complex molecules like proteins. Present high-resolution AFM is capable of imaging the topography of insulating objects without the limitations imposed by tunneling and thus could be able to provide valuable data about the shape of a folded protein.[46] Local force fields, mapped with AFM, can provide chemical information; in combination with functionalized tips, this could address the question how much of the original functionality is present in vacuum.[47] Extended unfolded proteins immobilized, for instance, on the copper surface could be used to identify single AA using vibrational fingerprints from inelastic tunneling spectroscopy—the sequencing of an individual protein as the ultimate goal (see Supporting Information C, Figure S2).[48,49]

Apart from SPM, many other high-resolution techniques will benefit from the capability of sample preparation provided by ES-IBD. For instance, free electron lasers provide coherent X-ray pulses that are in principle capable of probing the structure of a single protein, a well prepared sample provided.[50] Similarly, transmission electron microscopy is capable of imaging individual atoms or molecules at submolecular resolution immobilized on a well-defined substrate.[51] Finally, the SPM data of proteins fully immobilized immediately after deposition are closely related to the structure of gas-phase protein ions and can thus complement IMS measurements to gain additional insights.[5,6]

Besides the analytical capabilities, 2D self-assembly of oligopeptide- or even protein chains is another vision arising from this study. Up to now peptide self-assembly at surfaces in vacuum was limited to mono- and dipeptides, due to limited thermal stability. Nevertheless, complex behavior and effects, such as chiral recognition, could be demonstrated.[52−54]

The self-assembly of the peptide strands into compact, albeit irregular, patches observed on the Au(111) surface illustrates the possibility of 2D folding. Unsurprisingly, the CytC sequence, which evolved to be folded in physiological solution, did not yield regular assemblies on surfaces. However, other sequences might do so.[43] Compact patches of CytC are formed by weak unspecific intrachain interactions and are thus only stable at low temperatures. However, this suggests that it might be possible to form deterministic structures at room temperature by exploiting a hierarchical self-assembly approach that leads to an overall stronger bonding in the folded structure. Finding appropriate sequences will require substantial theoretical and experimental effort, yet it promises to add to the understanding of self-assembly by folding as well as opening the possibility for protein-like 2D functional structures at surfaces.

Methods. For deposition and in situ characterization in UHV we used our ES-IBD source[20,21] in situ connected to a variable temperature STM (Omicron VT-STM, Omicron Nanotechnology GmbH, Germany). The setup is described in Supporting Information A in more detail.

CytC (Aldrich D7752) was dissolved in solutions of water or water/methanol mixtures to which formic acid (FA, Fluka 94318) was later added. From these solutions, CytC gas-phase ions are created by pneumatically assisted ESI at a flow rate of 1 mL/h. The ions are transferred into vacuum and guided through six differentially pumped stages to reach a pressure below 10^{-10} mbar at the sample position. A rf-quadrupole ion guide in the third pumping stage is used to select the required m/z-section of the protein ion beam, which is monitored by the time-of-flight mass spectrometer downstream. On the substrate position in UHV, mass selected ion currents of 20−100 pA were detected and decelerated to a kinetic energy of 2−5 eV per charge before deposition. The coverage is monitored via a current measurement at the sample position using electrometers (Keithley 617).

Three different surfaces were used for deposition: Cu(001), Au(111), and BN/Rh(111). All surfaces were prepared in an integrated UHV preparation setup at a base pressure of 3×10^{-10} mbar. The metal crystals were repeatedly sputtered by argon ions and annealed. The BN nanomesh on the Rh(111) surface was prepared by purging the sample at 1300 K with 10^{-6} mbar borazine gas ($B_3N_3H_6$). The samples are transferred in situ to the deposition chamber and subsequently to the STM without ever breaking the ultrahigh vacuum.

■ ASSOCIATED CONTENT

Supporting Information

Detailed description of the ion beam deposition apparatus (A), the full description of the statistical analysis of the unfolded proteins (B) as well as additional data on bias dependent contrast (C), the protein BSA (D), and molecular dynamics simulations (E). This material is available free of charge via the Internet at http://pubs.acs.org.

■ AUTHOR INFORMATION

Corresponding Author

*E-mail: s.rauschenbach@fkf.mpg.de.

dx.doi.org/10.1021/nl3005385 | *Nano Lett.* XXXX, XXX, XXX−XXX

Notes

The authors declare no competing financial interest.

■ ACKNOWLEDGMENTS

The authors thank G. Cooks, I. Plazman, R. Gutzler, and J. Blohm for a critical reading of the manuscript and S. Buckenmaier for fruitful discussions about protein mass spectrometry.

■ REFERENCES

(1) Gething, M. J.; Sambrook, J. *Nature* **1992**, *355*, 33−45.
(2) Hartl, F. U. *Nature* **1996**, *381*, 571−580.
(3) Zhu, H.; Bilgin, M.; Bangham, R.; Hall, D.; Casamayor, A.; Bertone, P.; Lan, N.; Jansen, R.; Bidlingmaier, S.; Houfek, T.; Mitchell, T.; Miller, P.; Dean, R. A.; Gerstein, M.; Snyder, M. *Science* **2001**, *293*, 2101−2105.
(4) Fenn, J. B.; Mann, M.; Meng, C. K.; Wong, S. F.; Whitehouse, C. M. *Science* **1989**, *246*, 64−71.
(5) Clemmer, D.; Jarrold, M. F. *J. Mass Spectrom.* **1997**, *32*, 577−592.
(6) Kanu, A. B.; Dwivedi, P.; Tam, M.; Matz, L.; Hill, H. H. *J. Mass Spectrom.* **2008**, *43*, 1−22.
(7) Patterson, S. D.; Aebersold, R. H. *Nat. Genet.* **2003**, *33*, 311−323 198 Suppl. S.
(8) Abrahams, J. P.; Leslie, A. G. W.; Lutter, R.; Walker, J. E. *Nature* **1994**, *370*, 621−628.
(9) Frank, J.; Verschoor, A.; Boublik, M. *Science* **1981**, *214*, 1353−1355.
(10) van Heel, M.; Gowen, B.; Matadeen, R.; Orlova, E. V.; Finn, R.; Pape, T.; Cohen, D.; Stark, H.; Schmidt, R.; Schatz, M.; Patwardhan, A. *Q. Rev. Biophys.* **2000**, *33*, 307−369.
(11) Binnig, G.; Rohrer, H.; Gerber, C.; Weibel, E. *Phys. Rev. Lett.* **1983**, *50*, 120−123.
(12) Giessibl, F. J. *Rev. Mod. Phys.* **2003**, *75*, 949−983.
(13) Gimzewski, J. K.; Joachim, C. *Science* **1999**, *283*, 1683−1688.
(14) Miller, S. A.; Luo, H.; Pachuta, S. J.; Cooks, R. G. *Science* **1997**, *275*, 1447−1450.
(15) Grill, V.; Shen, J.; Evans, C.; Cooks, R. G. *Rev. Sci. Instrum.* **2001**, *72*, 3149−3179.
(16) Ouyang, Z.; Takats, Z.; Blake, T. A.; Gologan, B.; Guymon, A. J.; Wiseman, J. M.; Oliver, J. C.; Davisson, V. J.; Cooks, R. G. *Science* **2003**, *301*, 1351−1354.
(17) Gologan, B.; Green, J. R.; Alvarez, J.; Laskin, J.; Cooks, R. G. *Phys. Chem. Chem. Phys.* **2005**, *7*, 1490−1500.
(18) Laskin, J.; Wang, P.; Hadjar, O. *Phys. Chem. Chem. Phys.* **2008**, *10*, 1079 −1090.
(19) Johnson, G. E.; Hu, Q.; Laskin, J. *Annu. Rev. Anal. Chem.* **2011**, *4*, 83−104.
(20) Rauschenbach, S.; Vogelgesang, R.; Malinowski, N.; Gerlach, J. W.; Benyoucef, M.; Costantini, G.; Deng, Z.; Thontasen, N.; Kern, K. *ACS Nano* **2009**, *3*, 2901−2910.
(21) Thontasen, N.; Levita, G.; Malinowski, N.; Deng, Z.; Rauschenbach, S.; Kern, K. *J. Phys. Chem. C* **2010**, *114*, 17768−17772.
(22) Kahle, S.; Deng, Z.; Malinowski, N.; Tonnoir, C.; Forment-Aliaga, A.; Thontasen, N.; Rinke, G.; Le, D.; Turkowski, V.; Rahman, T. S.; Rauschenbach, S.; Ternes, M.; Kern, K. *Nano Lett.* **2012**, *12*, 518−521.
(23) Rauschenbach, S.; Stadler, F. L.; Lunedei, E.; Malinowski, N.; Koltsov, S.; Costantini, G.; Kern, K. *Small* **2006**, *2*, 540−547.
(24) Volny, M.; Elam, W. T.; Branca, A.; Ratner, B. D.; Turecek, F. *Anal. Chem.* **2005**, *77*, 4890−4896.
(25) Fuerstenau, S. D.; Benner, W. H.; Thomas, J. J.; Brugidou, C.; Bothner, B.; Siuzdak, G. *Angew. Chem., Int. Ed.* **2001**, *40*, 982−982.
(26) Alvarez, J.; Cooks, R. G.; Barlow, S. E.; Gaspar, D. J.; Futrell, J. H.; Laskin, J. *Anal. Chem.* **2005**, *77*, 3452−3460.
(27) Wang, P.; Laskin, J. *Angew. Chem., Int. Ed.* **2008**, *47*, 6678−6680.
(28) Volny, M.; Sengupta, A.; Wilson, C. B.; Swanson, B. D.; Davis, E. J.; Turecek, F. *Anal. Chem.* **2007**, *79*, 4543−4551.
(29) Laskin, J.; Wang, P.; Hadjar, O. *J. Phys. Chem. C* **2010**, *114*, 5305−5311.
(30) Saywell, A.; Magnano, G.; Satterley, C. J.; Perdigão, L. M. A.; Britton, A. J.; Taleb, N.; Giménez-López, M. d. C.; Champness, N. R.; O'Shea, J. N.; Beton, P. H. *Nat. Commun.* **2010**, *1*, 6355−6368.
(31) Sono, M.; Roach, M.; Coulter, E.; Dawson, J. *Chem. Rev.* **1996**, *96*, 2841−2887.
(32) Green, D.; Reed, J. *Science* **1998**, *281*, 1309−1312.
(33) Gaskell, S. J. *J. Mass Spectrom.* **1997**, *32*, 677−688.
(34) Clemmer, D. E.; Hudgins, R. R.; Jarrold, M. F. *J. Am. Chem. Soc.* **1995**, *117*, 10141−10142.
(35) Konermann, L.; Douglas, D. J. *Biochemistry* **1997**, *36*, 12296−12302.
(36) McLafferty, F.; Guan, Z.; Haupts, U.; Wood, T.; Kelleher, N. *J. Am. Chem. Soc.* **1998**, *120*, 4732−4740.
(37) Barth, J. V.; Brune, H.; Ertl, G.; Behm, R. J. *Phys. Rev. B* **1990**, *42*, 9307−9318.
(38) Zhang, J.; Sessi, V.; Michaelis, C. H.; Brihuega, I.; Honolka, J.; Kern, K.; Skomski, R.; Chen, X.; Rojas, G.; Enders, A. *Phys. Rev. B* **2008**, *78*, 165430.
(39) Bushnell, G. W.; Louie, G. V.; Brayer, G. D. *J. Mol. Biol.* **1990**, *214*, 585−595.
(40) Shelimov, K. B.; Jarrold, M. F. *J. Am. Chem. Soc.* **1996**, *118*, 10313−10314.
(41) Badman, E. R.; Myung, S.; Clemmer, D. E. *J. Am. Soc. Mass. Spectrom.* **2005**, *16*, 1493−1497.
(42) Horn, D.; Breuker, K.; Frank, A.; McLafferty, F. *J. Am. Chem. Soc.* **2001**, *123*, 9792−9799.
(43) Wolynes, P. G. *Proc. Natl. Acad. Sci. U. S. A.* **1995**, *92*, 2426−2427.
(44) Tkatchenko, A.; Rossi, M.; Blum, V.; Ireta, J.; Scheffler, M. *Phys. Rev. Lett.* **2011**, *106*, 118102.
(45) Harnau, L.; Winkler, R. G.; Reineker, P. *J. Chem. Phys.* **1996**, *104*, 6355−6368.
(46) Giessibl, F. J. *Appl. Phys. Lett.* **2000**, *76*, 1470−1472.
(47) Gross, L.; Mohn, F.; Moll, N.; Liljeroth, P.; Meyer, G. *Science* **2009**, *325*, 1110−1114.
(48) Stipe, B. C.; Rezaei, M. A.; Ho, W. *Science* **1998**, *280*, 1732−1735.
(49) Tanaka, H.; Kawai, T. *Nat. Nanotechnol.* **2009**, *4*, 518−522.
(50) Chapman, H. N.; et al. *Nature* **2011**, *470*, 73−81.
(51) Meyer, J. C.; Girit, C. O.; Crommie, M. F.; Zettl, A. *Nature* **2008**, *454*, 319−322.
(52) Barlow, S.; Louafi, S.; Le Roux, D.; Williams, J.; Muryn, C.; Haq, S.; Raval, R. *Surf. Sci.* **2005**, *590*, 243−263.
(53) Schiffrin, A.; Riemann, A.; Auwarter, W.; Pennec, Y.; Weber-Bargioni, A.; Cvetko, D.; Cossaro, A.; Morgante, A.; Barth, J. V. *Proc. Natl. Acad. Sci. U.S.A.* **2007**, *104*, 5279−5284.
(54) Lingenfelder, M.; Tomba, G.; Costantini, G.; Ciacchi, L. C.; De Vita, A.; Kern, K. *Angew. Chem., Int. Ed.* **2007**, *46*, 4492−4495.

dx.doi.org/10.1021/nl3005385 | *Nano Lett.* XXXX, XXX, XXX−XXX